

Supporting Information

Graphdiyne supported Ag-Cu tandem catalytic scheme for electrocatalytic reduction of CO₂ to C₂₊ products

Qiuying Zhu,^a Yuying Hu,^a Hongyu Chen,^b Chen Meng,^a Yizhu Shang,^a Chengcheng Hao,^a Shuxian Wei,^b Zhaojie Wang,^a Xiaoqing Lu^a and Siyuan Liu*^a

^a School of Materials Science and Engineering, China University of Petroleum, No.66 Changjiang West road, Huangdao District, Qingdao, Shandong 266580, P. R. China

^b College of Science, China University of Petroleum, No.66 Changjiang West road, Huangdao District, Qingdao, Shandong 266580, P. R. China

*E-mail: lsy@upc.edu.cn

Materials: All reagents were of analytical grade and used as received, unless otherwise noted. THF was freshly distilled from sodium under Ar. Sinopharm Chemical Reagent Co., Ltd. supplied the potassium hydrogen carbonate (KHCO₃), silver acetate (CH₃COOAg), ethanol and acetone. Shanghai Macklin Biochemical Technology Co., Ltd. provided tetrabutylammonium fluoride (TBAF) and cuprous iodide (CuI). Alfa Aesar provided Nafion N-115 membranes (0.180 mm thick, 0.90 meq g⁻¹ exchange capacity) as well as Nafion D-521 dispersion (5 percent w/w in water and 1-propanol, 0.92 meq g⁻¹ exchange capacity liquid). Without any further purification, all reagents were used as purchased. A Millipore Milli-Q water purification system was used to obtain deionized water.

Synthesis of catalysts Cu/GDY: The catalysts were made using the Schlenk process in an argon environment that was dry and oxygen-free. To a solution of hexamethyl[(trimethylsilyl)ethynyl]benzene (218 mg, 0.33 mmol) in dry THF (50 ml) was slowly added 2 ml TBAF (1.0 M in THF, 0.4 mmol) dropwise at low temperature, and stirred at -78 °C for 30 min. The solution was transferred to a suspension of cuprous iodide (375 mg, 1.969 mmol) in dry THF (10 ml). With vigorous stirring, the mixture was warmed to room temperature and heated with stirring at 60°C for 7 days. The precipitate was separated by centrifugation, and the product was sonicated in DMF at 40° C for 10 min, then washed with acetone, water, and ethanol in sequence, and dried in vacuo to obtain a brown powder.

Synthesis of catalysts Ag-Cu/GDY: Added 9.72 mg of silver acetate and 6.7 mg of imidazole to 8

ml of water and stirred to form a solution, took 0.99 ml, slowly added the suspension formed by Cu/GDY (15 mg) heated to 50°C and deionized water (10 ml) dropwise with stirring, and kept stirring at 50 °C (11,000 rpm) for 1 hour. Washed thoroughly with n-hexane/ethanol (1:1 by volume).

Computational methods: All calculations were performed by density functional theory (DFT) with the Vienna Ab initio Simulation Package (VASP).¹ The electron-ion interactions were represented by the projector-augmented-wave (PAW) potentials. The Perdew-Burke-Ernzerhof (PBE) exchange-correlation functional within a generalized gradient approximation (GGA) was used in this study. The k-points were set to be $3 \times 3 \times 1$ for geometry optimization and the 400 eV plane wave energy cutoff was used for all the computations. The electronic energy and forces were converged to within 10^{-5} and 0.02 eV/Å, respectively. A dispersion correction by DFT-D3 method with the standard parameters were employed to describe the van-der-Waals (VDW) interactions between the reaction intermediates and the catalysts.² GDY was described by a monolayer slab with a vacuum layer of 10 Å. The dispersive interaction was treated with the DFT+D3 scheme.³ Free energy corrections (including the zero-point energy, enthalpy, and entropy contributions) were included in the harmonic approximation.⁴ The gas-phase molecules were treated as ideal gases.

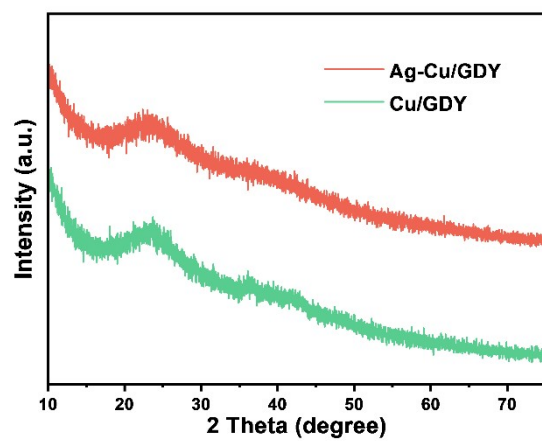


Figure S1. XRD patterns of Ag-Cu/GDY and Cu/GDY.

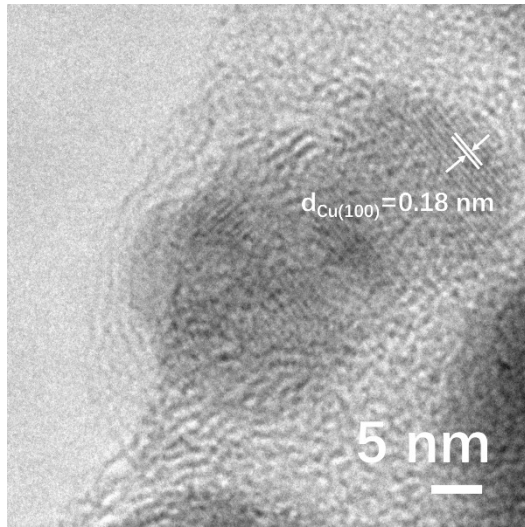


Figure S2. HR-TEM images of Ag-Cu/GDY.

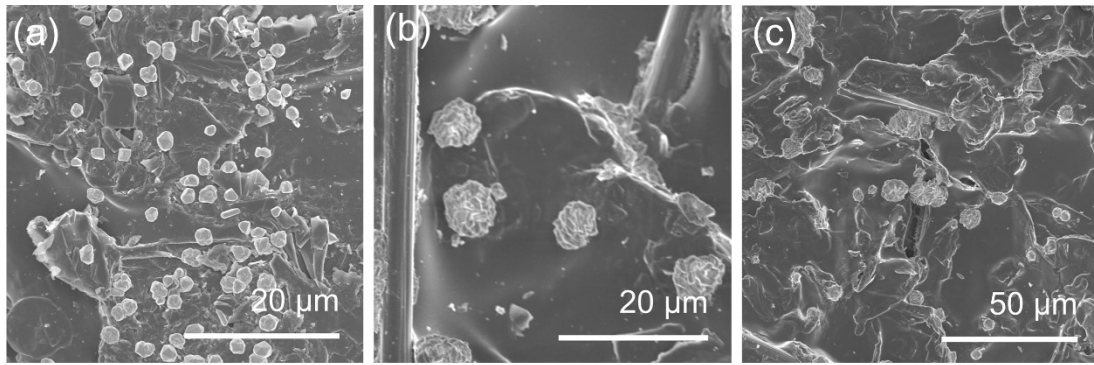


Figure S3. SEM images of electrodeposition on hydrophilic carbon paper at constant current (20 mA) for 5min, 10min and 15min respectively in 0.1M $\text{CuSO}_4 \cdot 5\text{H}_2\text{O}$ solution.

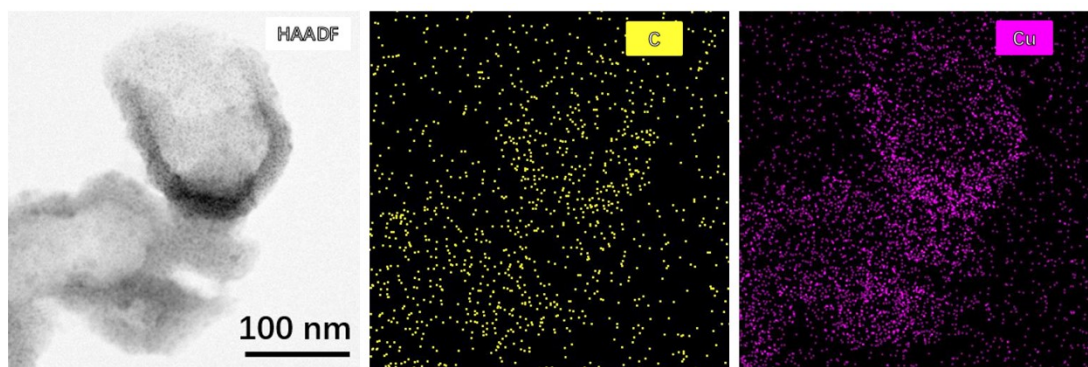


Figure S4. HADF image and its corresponding EDX images of Cu/GDY.

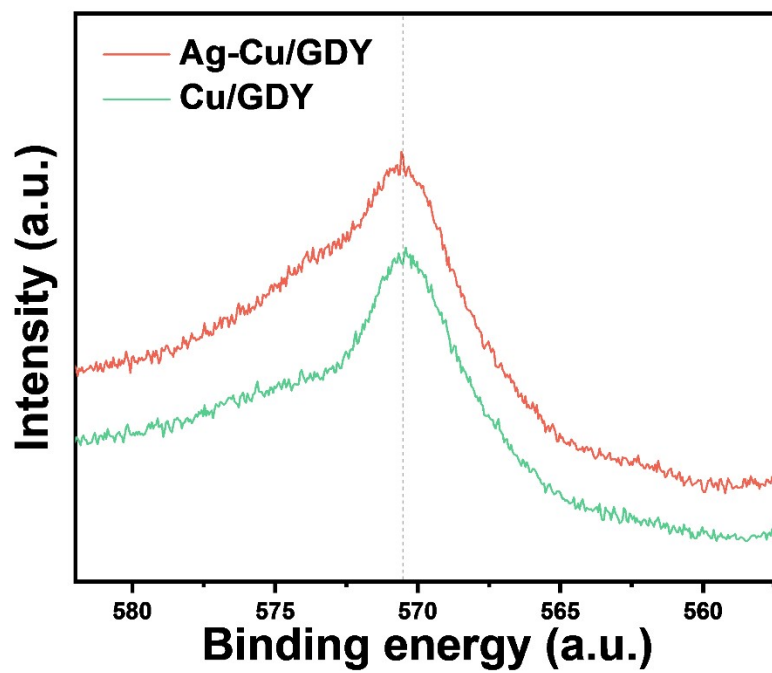


Figure S5. Cu LMM Auger spectra of Ag-Cu/GDY and Cu/GDY.

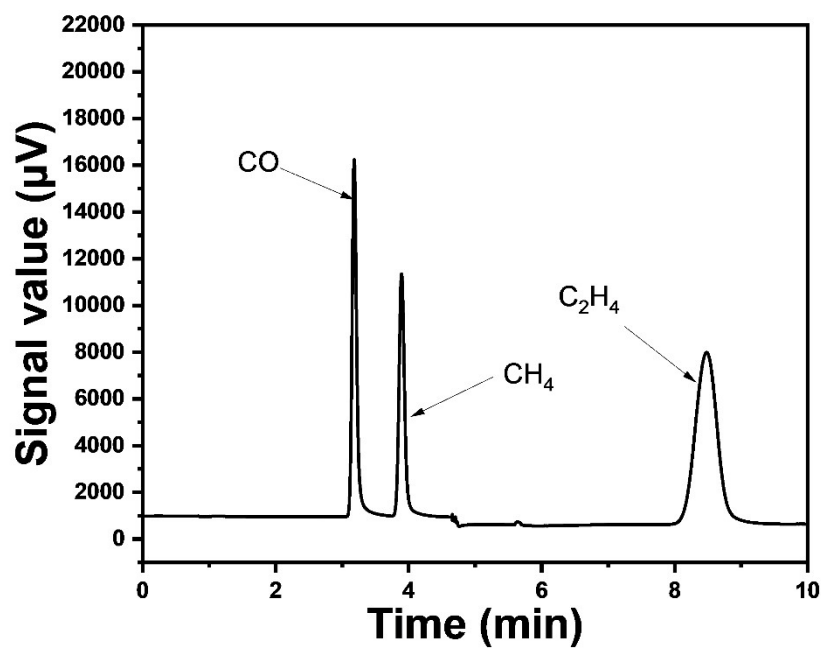


Figure S6. GC spectrum of carbon containing products in gas phase at -1.8 V.

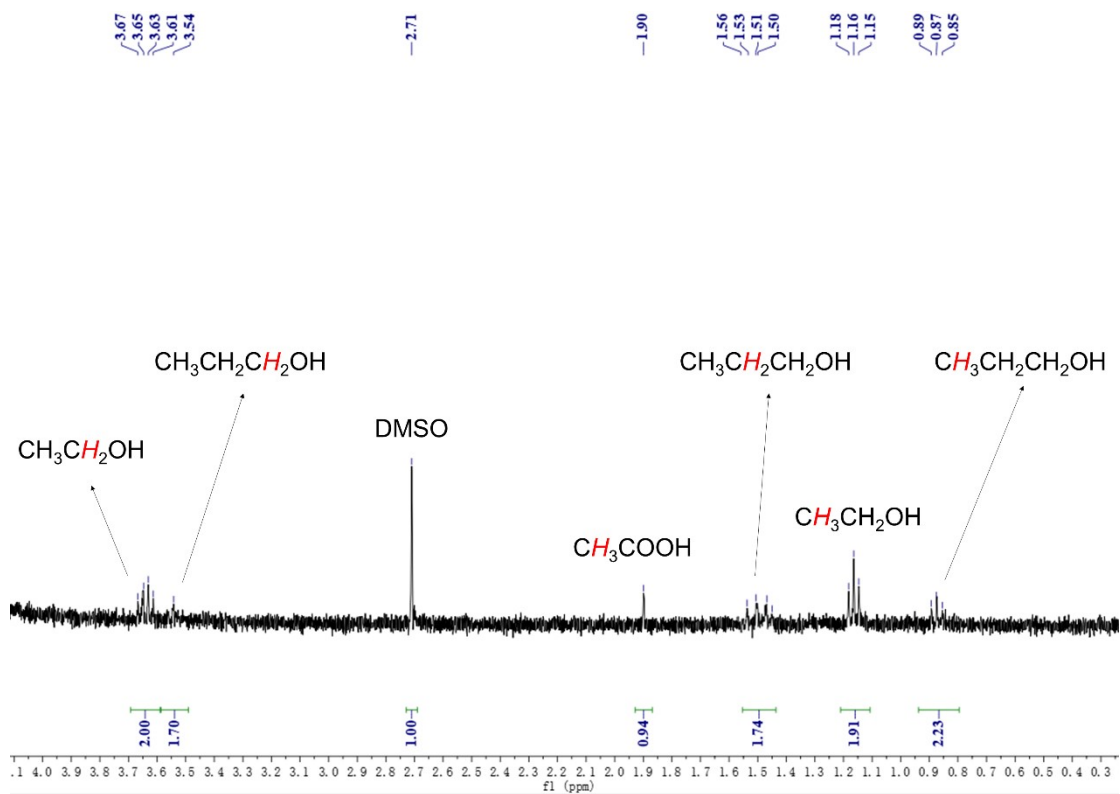


Figure S7. NMR spectra of carbon containing products in liquid phase at -1.8 V.

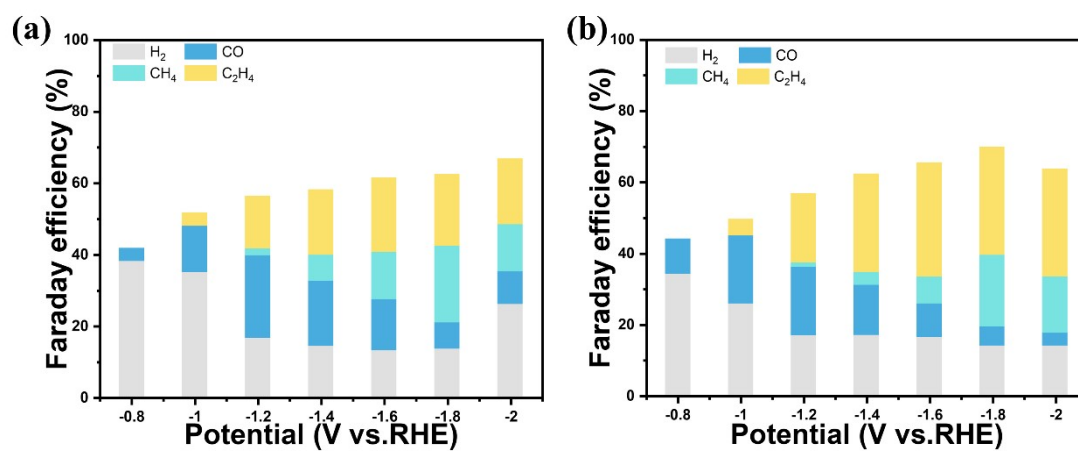


Figure S8. FE of a) Ag-Cu/GDY-0.5 and b) Ag-Cu/GDY-1.5.

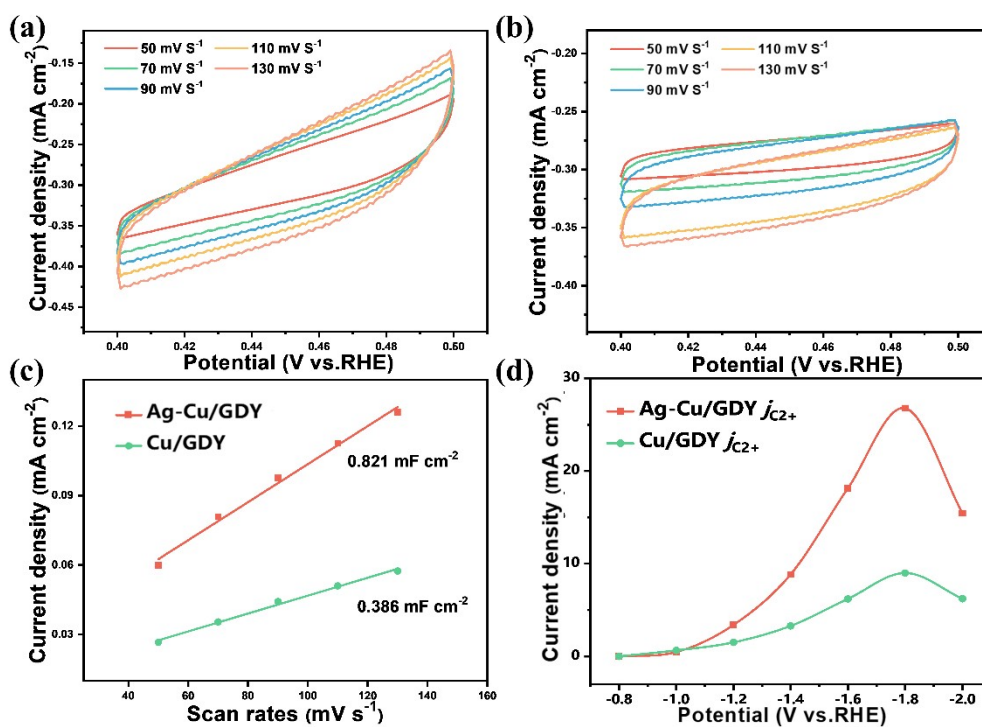


Figure S9. Cyclic voltammetry scans on a) Ag-Cu/GDY, b) Cu/GDY between 0.41 and 0.51 V in CO_2 -saturated 0.1 M KHCO_3 solution at scan rates of 50, 70, 90, 110, and 130 mV s^{-1} ; c) Extracted currents at 0.5 V as a function of the scan rate; leading that the half of the slope is calculated as double layer capacitance (C_{dl}); d) Partial current density of Ag-Cu/GDY and Cu/GDY samples with different chemical compositions.

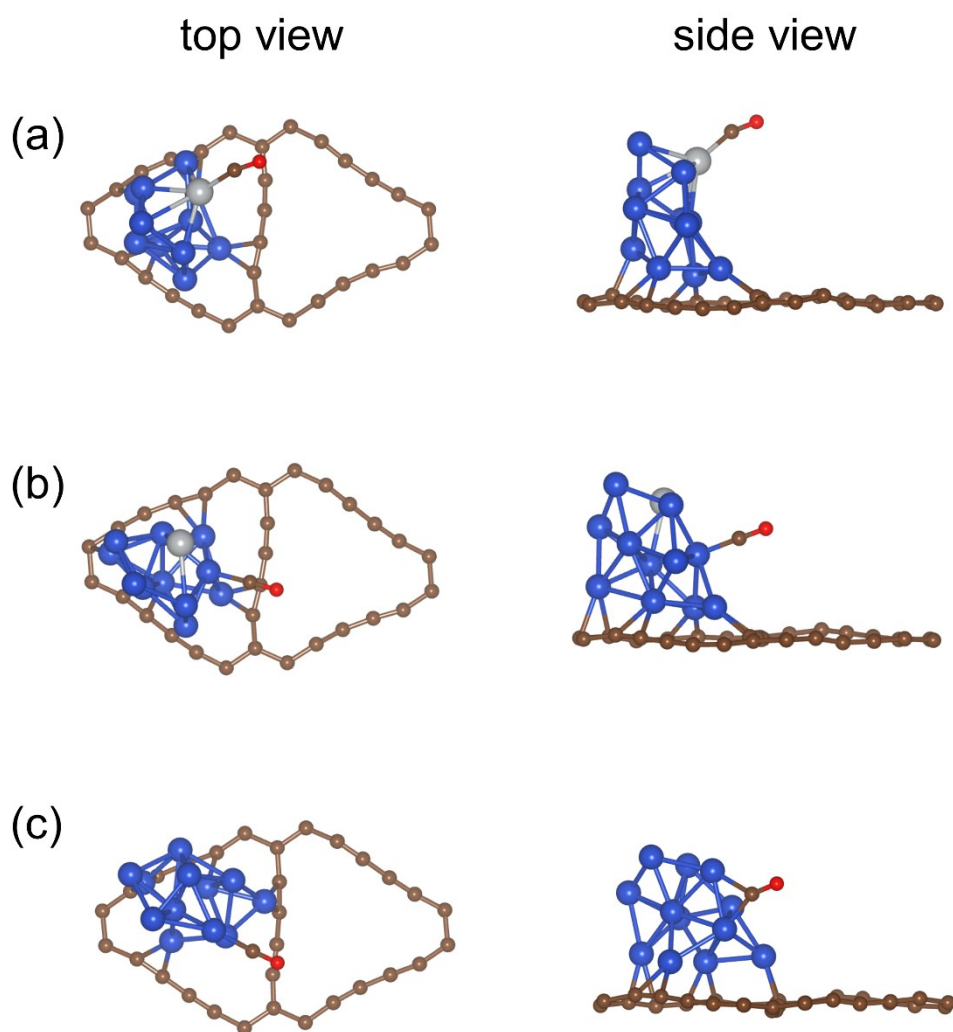


Figure S10. CO adsorption models at a) Ag sites, b) Cu sites of Ag-Cu/GDY, and c) Cu sites of Cu/GDY.

Table S1. Determination of Actual molar ratios and actual metal loadings of Ag/Cu on catalysts by inductively coupled plasma optical emission spectroscopy (ICP-OES) analysis.

Catalysts	Cu wt.%	Ag wt.%	Ag/Cu molar ratio
Cu/GDY	33.8785	0	
Ag-Cu/GDY	30.5122	0.7706	1.487%
Ag-Cu/GDY-1.5	29.5376	1.4473	2.886%
Ag-Cu/GDY-0.5	30.9179	0.4287	0.817%

Table S2. Double-layer capacitance of different electrodes and corresponding normalized roughness factor.

Electrodes	C_{dl} (mF cm⁻²)	R_f
Cu/GDY	0.386	1
Ag-Cu/GDY	0.821	2.13

Table S3. Summary of the catalysts for the coordinated electro catalytic reduction of CO₂ to C₂₊ by Ag-Cu were reviewed.

Electrocatalysts	Potentials (V vs. RHE)	j (mA cm ⁻²)	FE (%)	Ref.
Ag-Cu/GDY	-1.8	j_{C2+}=24.98	55.1	This work
Cu@Ag NPs	-2.25	j _{C2+} =47.3	43	5
Ag/Cu nanocrystals	-1.1	j _{C2H4} ~3.6	40	6
Ag@Cu Np	-0.5	j _{C2H4} ~8.1	41.3	7
Plasmonically active copper– silver cathode	-1.0	j _{C2H4} ~1	~23	8
Cu ₉₅ Ag ₅	-0.85	j _{C2+} ~15	~30	9
Cu _{8.2} Ag _{1.8} NWs	-1.13	j _{C2+} ~1	25.06	10
Cu ₅₀₀ Ag ₁₀₀₀	-0.7	j _{C2+} ~160	50	11

References:

- 1 G. Kresse and J. Furthmüller, *Phys. Rev. B*, 1996, **54**, 11169.
- 2 J. P. Perdew, K. Burke and M. Ernzerhof, *Phys. Rev. Lett.*, 1996, **77**, 3865.
- 3 S. Grimme, S. Ehrlich and L. Goerigk, *J. Comput. Chem.*, 2011, **32**, 1456-1465.
- 4 A. A. Peterson, F. Abild-Pedersen, F. Studt, J. Rossmeisl and J. K. Nørskov, *Energy Environ. Sci.*, 2010, **3**, 1311-1315.
- 5 A. N. Kuhn, H. Zhao, U. O. Nwabara, X. Lu, M. Liu, Y. T. Pan, W. Zhu, P. J. Kenis and H. Yang, *Adv. Funct. Mater.*, 2021, **31**, 2101668.
- 6 J. Huang, M. Mensi, E. Oveisi, V. Mantella and R. Buonsanti, *J. Am. Chem. Soc.*, 2019, **141**, 2490-2499.
- 7 L. Hou, J. Han, C. Wang, Y. Zhang, Y. Wang, Z. Bai, Y. Gu, Y. Gao and X. Yan, *Inorg. Chem. Front.*, 2020, **7**, 2097-2106.
- 8 E. R. Corson, A. Subramani, J. K. Cooper, R. Kostecki, J. J. Urban and B. D. McCloskey, *Chem. Commun.*, 2020, **56**, 9970-9973.
- 9 Y. Xu, C. Li, Y. Xiao, C. Wu, Y. Li, Y. Li, J. Han, Q. Liu, and J. He, *ACS Appl. Mater. Interfaces*, 2022, **14**, 11567-11574.
- 10 C. Choi, J. Cai, C. Lee, H. M. Lee, M. Xu and Y. Huang, *Nano Res.*, 2021, **14**, 3497-3501.
- 11 C. Chen, Y. Li, S. Yu, S. Louisia, J. Jin, M. Li, M. B. Ross, P. Yang, *Joule*, 2020, **4**, 1688-1699.